Proc. Natl. Acad. Sci. USA
Vol. 94, pp. 13317–13322, November 1997
Physiology

G_i regulation of secretory vesicle swelling examined by atomic force microscopy

(zymogen granule dynamics/GTP/NaF/Mas7)

BHANU P. JENA*†, STEFAN W. SCHNEIDER*, JOHN P. GEIBEL*‡, PAUL WEBSTER§, HANS OBERLEITHNER¶, AND KUMUDESH C. SRITHARAN*

*Departments of Surgery, ‡Cellular and Molecular Physiology, and §Cell Biology, Yale University School of Medicine, New Haven, CT 06510; and ¶Department of Physiology, University of Würzburg, D-97070 Würzburg, Germany

Communicated by Robert W. Berliner, Yale University School of Medicine, New Haven, CT, August 29, 1997 (received for review March 12, 1997)

ABSTRACT **In the last decade, several monomeric and heterotrimeric guanine nucleotide binding proteins have been identified to associate with secretory vesicles and to be implicated in exocytosis. Vesicle volume also has been proposed to play a regulatory role in secretory vesicle fusion at the plasma membrane. However, the molecular mechanism of function of the guanine nucleotide binding proteins and of the regulation of secretory vesicle volume in the exocytotic process remains unclear. In this study, we report association of the secretory vesicle membrane with the α subunit of a heterotrimeric GTP binding protein $G_{\alpha i3}$ and implicate its involvement in vesicle swelling. Using an atomic force microscope in combination with confocal microscopy, we were able to study the dynamics of isolated zymogen granules, the secretory vesicles in exocrine pancreas. Exposure of zymogen granules to GTP resulted in a 15–25% increase in vesicle height as measured by the atomic force microscope and a similar increase in vesicle diameter as determined by confocal microscopy. Mas7, an active mastoparan analog known to stimulate G_i proteins, was found to stimulate the GTPase activity of isolated zymogen granules and cause swelling. Increase in vesicle size in the presence of GTP, NaF, and Mas7 were irreversible and KCl-sensitive. Ca^{2+} had no effect on zymogen granule size. Taken together, the results indicate that $G_{\alpha i3}$ protein localized in the secretory vesicle membrane mediates vesicle swelling, a potentially important prerequisite for vesicle fusion at the cell plasma membrane.**

Chemiosmotic forces have been proposed to play a regulatory role in exocytosis (1–3). According to the chemiosmotic hypothesis, osmotic swelling of secretory vesicles have been suggested to be critical in their fusion at the plasma membrane. It has been demonstrated that osmotic force is a requirement for fusion of phospholipid vesicles with a bilayer membrane (1). Vesicle volume increases after stimulation of secretion have been suggested from electrical measurements in mast cells (4–7). Studies using isolated zymogen granules (ZG) from the exocrine pancreas and parotid glands demonstrate the presence of Cl^- and ATP-sensitive K^+ selective ion channels at the vesicle membrane, whose activities were implicated in vesicle swelling (8–16). Furthermore, secretion of ZG contents in permeabilized pancreatic acinar cells require the presence of both K^+ and Cl^- ions (5). A major unknown, however, is the molecular mechanism regulating ZG-associated Cl^- and K^+ selective ion channels implicated in ZG swelling. The present study was undertaken to address this question.

Studies in the last decade suggest that GTP acting via monomeric (*ras*-like) and heterotrimeric GTP-binding proteins associated with secretory vesicles regulates exocytosis (17–20). Fluorimetric ZG-pancreatic plasma membrane (ZG-PPM) fusion studies in our laboratory and similar studies from other laboratories (21) demonstrate an increase in ZG-PPM fusion in the presence of GTP and NaF. These ZG-PPM fusion studies suggest the involvement of heterotrimeric GTP-binding proteins in ZG fusion at the plasma membrane. The heterotrimeric $G_{\alpha i3}$ protein has been implicated in regulation of both ATP-sensitive K^+ channels as well as Cl^- channels in several tissues (22–25), so the presence of similar G protein(s) in the ZG membrane (ZGM) and their involvement in vesicle swelling were investigated. To examine if monomeric GTP-binding proteins are involved in the regulation of vesicle size, the effect of NaF on vesicle dynamics was investigated. NaF is a potent stimulator of heterotrimeric GTP-binding proteins but has no effect on monomeric *ras*-like proteins. Therefore, studies using NaF help to dissociate the effects of heterotrimeric from monomeric GTP-binding proteins. Differences in GTP and NaF influence on vesicle size would suggest a role for *ras*-like proteins in the regulation of vesicle size.

Confocal microscopy was used to examine changes in ZG size after exposure to known regulators of secretion. Results obtained from confocal studies were confirmed further using an atomic force microscope (AFM). Three-dimensional images at nanomolar resolution of isolated ZGs were obtained by using the AFM in both the contact (26) and tapping modes in fluid (27–29).

MATERIALS AND METHODS

Isolation of ZGs and Preparation of ZGMs. ZGs were isolated by modification of a published procedure (30). Male Sprague–Dawley rats weighing 80–100 g were killed by ether inhalation for each ZG preparation. The pancreas was dissected and diced into 0.5-mm^3 pieces. The pieces of pancreas were suspended in 15% (wt/vol) ice-cold homogenization buffer (0.3 M sucrose/25 mM Hepes, pH 6.5/1 mM benzamidine/1 mM phenylmethylsulfonyl fluoride/0.01% soybean trypsin inhibitor) and homogenized using a Teflon glass homogenizer. The resultant homogenate was centrifuged for 5 min at 300 $\times$ *g* at 4°C to obtain supernatant. One volume of the above supernatant was mixed with 2 vol of a Percoll–Sucrose–Hepes buffer (0.3 M sucrose/25 mM Hepes, pH 6.5/86% Percoll/0.01% soybean trypsin inhibitor) and centrifuged for 30 minutes at 16,400 $\times$ *g* at 4°C. Pure ZGs, as visualized by electron microscopy (Fig. 1*a*) were obtained as a loose white pellet at the bottom of the tube. Isolated ZGs were

The publication costs of this article were defrayed in part by page charge payment. This article must therefore be hereby marked "*advertisement*" in accordance with 18 U.S.C. §1734 solely to indicate this fact.

Abbreviations: ZG, zymogen granule; ZGM, ZG membrane; TH, total pancreatic homogenate; AFM, atomic force microscope.

†To whom reprint requests should be addressed. e-mail: Bhanu.Jena@Yale.edu.

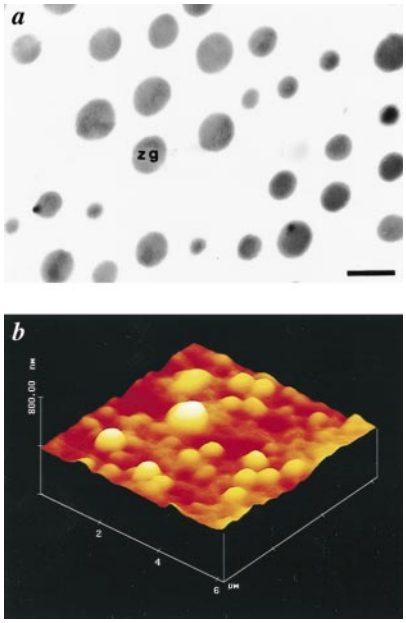

FIG. 1. Isolated ZGs ranging in size from 0.2 to 1.2 μm obtained from rat pancreas as seen by electron and AFM. (*a*) An electron micrograph of the electron-dense ZGs. Note the purity of the ZG preparation. (Bar = 1 μm.) (*b*) A three-dimensional AFM image of isolated ZGs adhering to a Cell-Tak-coated mica sheet. Notice the size heterogeneity in the ZG population.

washed three times and resuspended in 125 mM ice-cold 2-Mes buffer (pH 6.5). ZGM was prepared by the method of Cameron and Castle (31).

Electron Microscopy of Isolated ZGs. Washed ZGs were resuspended for 4 h at 4°C in 125 mM Mes buffer (pH 6.5) containing 4% paraformaldehyde. After fixation, the ZGs were pelleted and embedded in 12% aqueous gelatin, infiltrated in 2.1 M sucrose containing 20% poly(vinyl) pyrolidone, and frozen by immersion in liquid nitrogen and cryosectioned (32). The frozen sections were transferred to coated specimen grids, dried in the presence of uranyl acetate and methyl cellulose, and examined in a Philips 410 transmission electron microscope.

Single Dimension SDS/PAGE and Western Blot Analysis. Protein concentrations in the preparations were assayed by the Bradford method (33). Ten micrograms of total pancreatic homogenate (TH) and purified ZGM was resolved using 12.5% SDS/PAGE). The resolved proteins were electrotransfered to 0.2-μm nitrocellulose membranes and immunoblotted with $G_{\alpha s}$-, $G_{\alpha i3}$-, $G_{\alpha z}$-, and $G_{\alpha t}$-specific antibody (1:1000) followed by horseradish peroxidase-conjugated secondary antibody (1:1000). The immunoblots were then processed for the enhanced chemiluminescence reaction and exposed to X-Omat-AR film. The exposed film was then developed and photographed.

Two-Dimensional 16-BAC Gel and Western Blot Analysis. The purified ZGM (25 μg) was resolved by the published two-dimensional 16-benzyldimethyl-*n*-hexadecylammonium chloride-SDS/PAGE method (34). The resolved proteins were electrotransfered to 0.2-μm nitrocellulose membranes, immunoblotted with the $G_{\alpha i3}$-specific antibody, and processed for enhanced chemiluminescence as described earlier.

Measurement of GTPase Activity in Isolated ZGs. GTPase activity was measured by minor modification of a published procedure (35). Reaction was initiated by the addition of 20 μg of ZG (GTPase source) to 100 μl of the following reaction buffer: 25 mM Hepes, pH 6.5/1 mM DTT/1 mM EGTA/20 mM $MgCl_2$/1 mM ATP/1 mM adenylyl imidodiphosphate/5 mM creatine phosphate/0.2 mg/ml creatine phosphokinase/

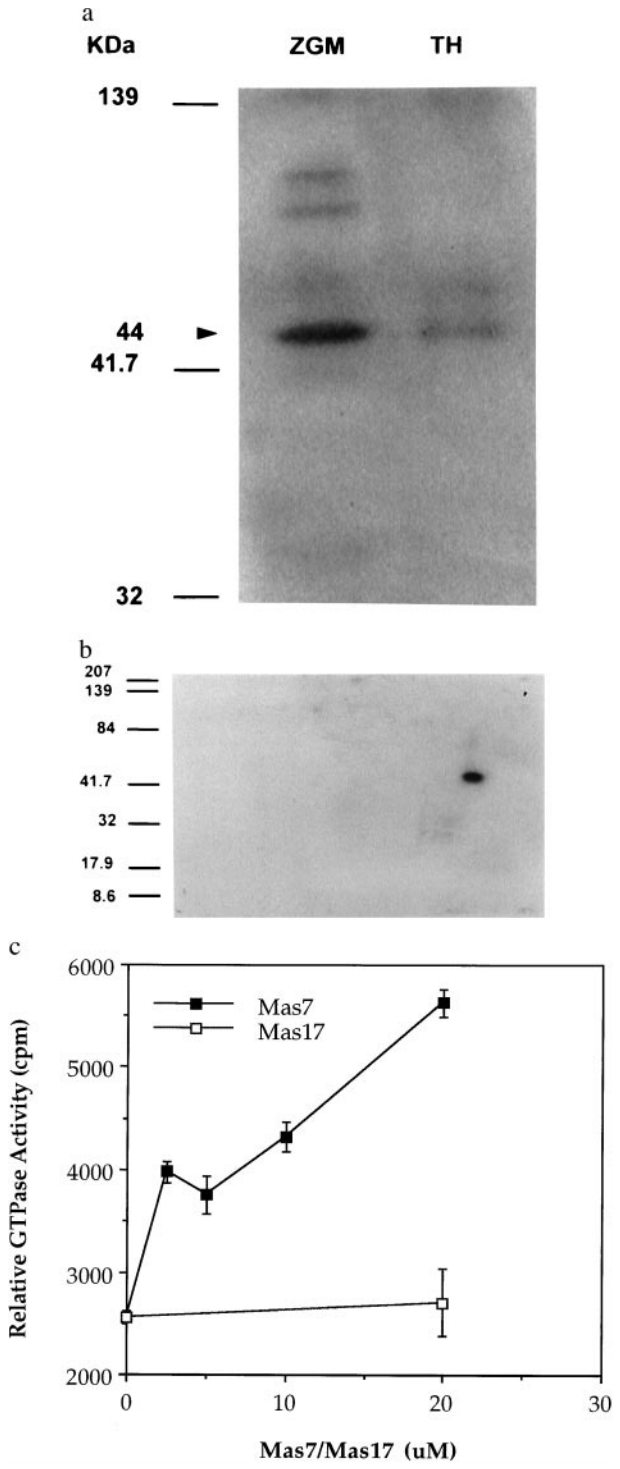

FIG. 2. Immunolocalization and biochemical detection of a G_i protein with ZGs from rat exocrine pancreas. (*a* and *b*) Immunoblot analysis. Identification of $G_{\alpha i3}$-immunoreactive antigen associated with ZGM. (*a*) Ten micrograms each of TH and ZGM was resolved using a single dimension 12.5% SDS gel electrophoresis before electrotransfer on to nitrocellulose and immunoblotting. A 44-kDa immunoreactive band was detected in both fractions but enriched in the ZGM. (*b*) Twenty five micrograms of ZGM protein was resolved on two-dimensional 16-BAC gel electrophoresis before electrotransfer and immunoblotting using the $G_{\alpha i3}$-specific antibody. Note a single spot at ≈44 kDa, suggesting that only one $G_{\alpha i3}$ isoform is present in the ZGM. (*c*) Detection of G_i-specific GTPase activity associated with ZG. GTPase activity in 25 μg of ZG incubated at 30°C for 5 min in the presence of varying concentrations of either Mas7 or Mas17 demonstrates a dose-dependent increase in activity in the presence of Mas7, which is absent in the presence of Mas17. Values are mean ± SE.

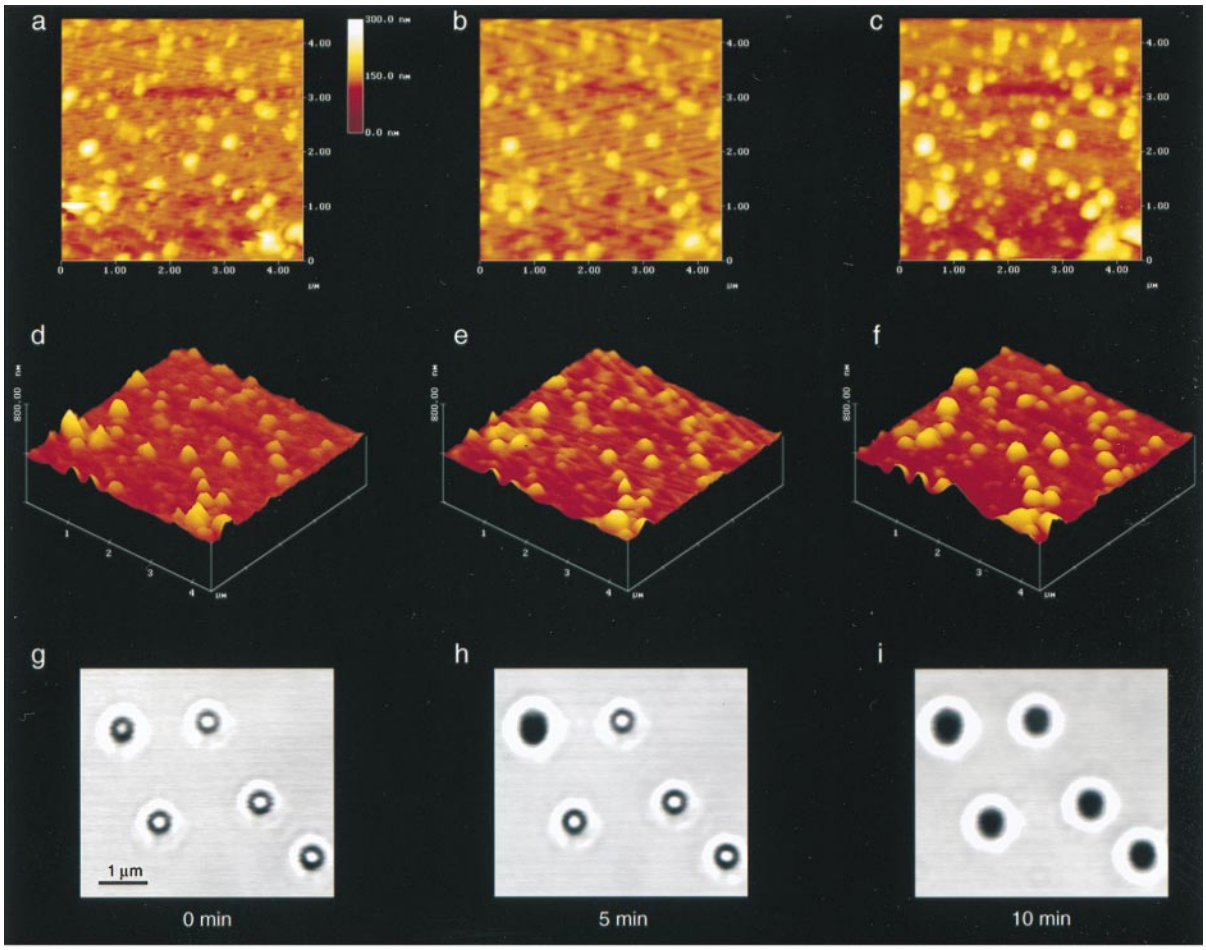

FIG. 3. Increase in size of ZGs in the presence of GTP. (*a–c*) Two-dimensional AFM images of the same granules after exposure to 20 μM GTP at time 0 (*a*), 5 minutes (*b*), and 10 minutes (*c*). (*d–f*) The same granules are shown in three-dimensions: the three-dimensional image of the granules at time 0, 5 minutes, and 10 minutes, respectively, after exposure to GTP. (*g-i*) The GTP-induced increase in size of another group of ZGs observed by confocal microscopy. Confocal images of the same ZGs at time 0, 5 minutes, and 10 minutes after GTP exposure are shown. (Bar = 1 μm.) Values represent one of three representative experiments.

0.2% BSA/100nM [γ-^{32}P]GTP. Reactions were carried out in 1.5-ml screw cap Eppendorf tubes in a 30°C shaking-water bath for 10 min. The reaction was stopped by adding 900 ml of ice-cold trichloroacetic acid (pH 2.0) supplemented with 5% charcoal by weight. The mixture was thoroughly vortexed and centrifuged at 10,000 × *g* for 30 min at 4°C. ^{32}P in the supernatant was quantitated by liquid scintillation. Blanks in the presence of the 100 nM [γ-^{32}P]GTP were run routinely and subtracted from the assay to determine the GTPase activity in the experimental tubes.

Preparation of ZGs for AFM and Confocal Microscopy. For AFM, isolated, washed ZG suspensions in 125 mM Mes buffer (pH 6.5) were plated on Cel-Tak-coated (cell and tissue adhesive), freshly cleaved mica sheets (Collaborative Biomedical Products, Bedford, MA). Fifteen minutes after plating, the mica sheets with attached ZGs were washed in 125 mM Mes buffer (pH 6.5) to remove unattached granules. ZGs attached to the surface of the mica sheet were placed in a fluid chamber containing 2 ml of the appropriate buffer at room temperature and were visualized using an inverted optical microscope for probe positioning before being imaged by the AFM. For confocal microscopy, isolated, washed ZG suspension in 125 mM Mes buffer (pH 6.5) was plated on Cel-Tak-coated glass coverslips and placed in the fluid chamber. GTP, NaF, Mas7, Mas17, Ca^{2+}, or EGTA was added to the buffer in the fluid chamber, and their effect on ZG size was monitored with time. To study the role of Cl^- and K^+ ions on vesicle swelling, the influence of GTP, Mas7, Mas17, Ca^{2+}, or EGTA on ZG size was assessed in KCl (25 mM KCl/100 mM Mes buffer, pH 6.5) and KCl-free buffers (25 mM cyclamide/100 mM Mes buffer, pH 6.5). Furthermore, to determine if ZG-associated monomeric GTP-binding proteins were involved in ZG size regulation, the effects of GTP and NaF on ZG size were compared.

AFM. ZGs were imaged using AFM (BioScope Digital Instruments, Santa Barbara, CA) in both "contact" and "tapping" modes in fluid (27–29). However, all AFM images presented in this manuscript were obtained in the contact mode in fluid. Silicon nitride tips (Digital Instruments, Santa Barbara, CA) with a spring constant of 0.06 $N \cdot m^{-1}$ were used in the study. Images of the ZGs were obtained by the AFM BioScope (Fig. 1*b*) operating in the contact mode in fluid by using a very low vertical imaging force typically between 0.2 and 0.5 nN. All studies conducted in the contact mode in fluid were confirmed using the tapping mode in fluid, in which <200 pN of imaging force was applied. Force calibrations were made before and after acquiring each image to keep the imaging force applied on the ZGs constant. In addition, image gains were kept constant. AFM images were generated at line frequencies of 1–3 Hz, with 256 or 512 lines per image. GTP, Ca^{2+}, or EGTA was added to the perfusate in the fluid cell, and the responding time-dependent morphological changes of the ZGs were imaged. Images were stored either in the computer hard drive or in floppy disks. Topographical dimensions of ZGs were analyzed using the software supplied by Digital Instruments. The AFM and confocal microscope have

enabled us to examine the morphology of the same vesicles over time under different treatment conditions.

Confocal Microscopy in the Measurement of ZG Diameter. Freshly isolated ZGs in Mes, Mes-KCl, or Mes-cyclamide buffer (pH 6.5) were placed on Cel-Tak-coated glass coverslips. After allowing the ZGs to settle and adhere to the coverslips for 15 minutes, the preparation was washed with the appropriate buffer [Mes, Mes-KCl, or Mes-cyclamide buffer (pH 6.5)] five times (2 minutes each wash) and placed in a fluid chamber. The preparation was placed on the stage of an inverted oil emersion microscope, a part of the Carl Zeiss Laser Scanning Axiovert 100 Laser Scanning Microscope. Using a ×40 objective, transmitted images of control and experimental ZGs were obtained at various time intervals. Using the Axiovert 100 Laser Microscope software, the area and diameter of the ZGs were determined.

RESULTS

Purity and Size Heterogeneity of ZGs. The purity of ZGs was determined by imaging the isolated ZGs by using a transmission electron microscope. Fig. 1*a* is an electron micrograph of the purified electron dense ZGs with no detectable subcellular contaminants. When isolated ZGs plated on Cell-Tak-coated mica sheets were placed in 125 mM Mes buffer (pH 6.5) and imaged by the AFM, three-dimensional images were obtained (Fig. 1*b*) that demonstrated a size heterogeneity in the ZG population. Measurements of ZG images obtained by AFM demonstrated that the diameter of ZGs range from 0.2 to 1.2 μm.

Association of $G_{\alpha i3}$ with ZGM. Immunoblot analysis of pancreatic TH and ZGM fractions using a $G_{\alpha i3}$-specific antibody after resolution by SDS/PAGE and electrotransfer to nitrocellulose membrane demonstrated a 44-kDa major immunoreactive band in both fractions. An increase in band intensity was found in the ZGM fraction over TH (Fig. 2*a*). An affinity-purified rabbit polyclonal antibody (Santa Cruz Biotechnology) raised against a peptide corresponding to aa 345–354 mapping at the carboxy terminus of $G_{\alpha i3}$ of rat origin was used in the study. No immunoreactive bands were detected in the ZGM fraction when the nitrocellulose with resolved proteins was immunoblotted with affinity-purified $G_{\alpha s}$-, $G_{\alpha z}$-, and $G_{\alpha t}$-specific antibodies (not shown). To determine if more than one $G_{\alpha i}$ isoform was present in ZGM, two-dimensional 16-BAC gel followed by immunoblotting using the $G_{\alpha i3}$-specific antibody was performed. Results from this study demonstrate a single spot at approximately the 44-kDa mark to be present in ZGM (Fig. 2*b*). The 44-kDa immunoreactive band (single dimension protein resolution) or spot (two-dimensional protein resolution) was absent in blots that were immunostained with peptide-neutralized antibody (not shown).

Biochemical Determination of ZG-Associated G_i Protein(s). Mastoparan, an amphiphilic tetradecapeptide from wasp venom, has been demonstrated to activate the GTPase activity of G_i proteins (35–37). Stimulation of G proteins is believed to occur by the peptide inserting into the phospholipid membrane and forming a highly structured α-helix that resembles the intracellular loops of G protein-coupled receptors. Analogous to receptor activation, mastoparan is thought to interact with the COOH-terminal domain of the G protein α subunit (38). Active (Mas7) and inactive (Mas 17) analogs of mastoparan in the presence of [γ-^{32}P]GTP were used to determine the GTPase activity in ZGs. Our study demonstrates a significant increase in GTPase activity in ZG in the presence of Mas7 over control (Mas17), confirming the presence of G_i proteins with ZGs (Fig. 2*c*).

Vesicle Size Increase After Exposure to GTP. When isolated ZGs plated on Cel-Tak-coated mica sheets were placed in 100 mM Mes buffer (pH 6.5) and 25 mM KCl and exposed to 20 μM GTP for 10 minutes, a 15–25% increase in vesicle height (mean ± SE: 19.25 ± 4.05%) as measured by the ATM (Figs. 3 and 4) and a 20–30% increase in vesicle diameter (mean ± SE: 24.5 ± 5.4%) determined by confocal microscopy (Figs. 3 and 4) were observed. No further increase in vesicle size was observed after 10 minutes of GTP exposure or on exposure of ZGs to an increased GTP concentration of up to 100 μM. A similar increase in size of ZGs was observed in the presence of the nonhydrolyzable GTP analog GMP-P(NH)P but not in the presence of GDP (data not shown).

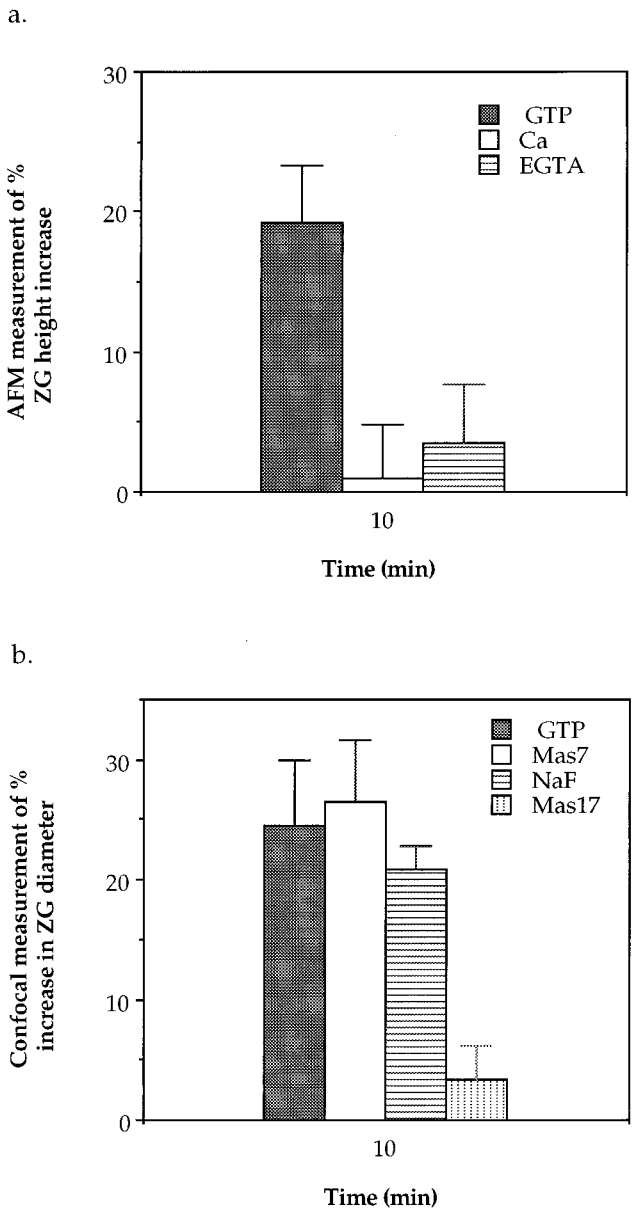

FIG. 4. Change in ZG height and diameter measured by AFM and confocal microscopy, respectively. (*a*) Increase in the height of isolated ZGs were observed only in the presence of GTP. Analysis of height change in various population of ZGs (n = 14) exposed for 0 minutes and the same ZGs exposed for 10 minutes to 20 μM GTP, 100 μM Ca^{2+}, or 200 μM EGTA is graphically depicted. A significant increase in ZG height was observed only in the GTP-exposed groups. Paired Student's t tests, with $P < 0.001$, were used. (*b*) Similar increases in ZG diameter as measured by the confocal microscope were observed in ZGs exposed to GTP, Mas7, and NaF. Change in diameter of various population of ZGs (n = 10), exposed to 20 μM GTP, 20 μM Mas7, or 100 μM NaF for 10 minutes is shown. A significant ($P < 0.001$) increase in ZG diameter at the 10-minute time point over the 0-minute time point is seen. Twenty micromolars of Mas17 (control) had no effect on ZG size. Values represent one of three representative experiments.

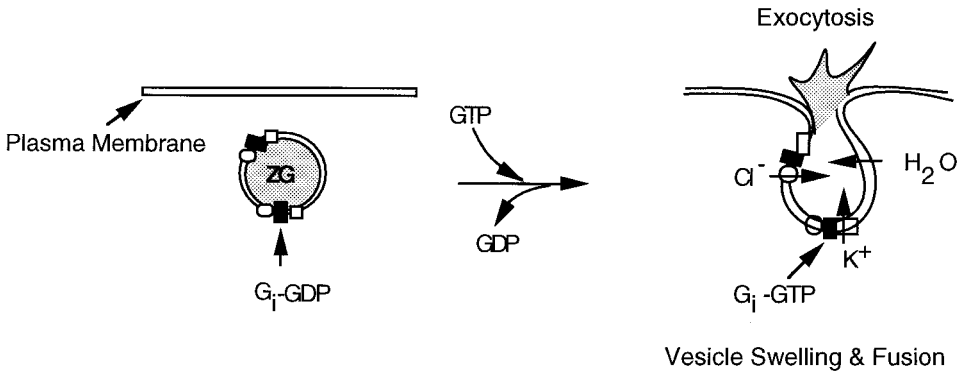

FIG. 5. Hypothetical model depicting the possible role of ZGM-associated $G_{\alpha i3}$ in regulation of secretory vesicle swelling and fusion at the plasma membrane in pancreatic acinar cells. In the presence of GTP, the $G_{\alpha i3}$ protein is activated by replacement of its GDP with GTP, resulting in the opening of ZGM-associated Cl^- and K^+ channels. There is then a net increase in flow of Cl^- and K^+ ions together with water molecules into the ZG lumen, resulting in vesicle swelling and subsequent fusion at the plasma membrane by an unknown mechanism.

ZG-Associated $G_{\alpha i3}$ May Mediate GTP Effects on Vesicle Swelling. Exposure of isolated ZGs to Mas7 in 100 mM Mes buffer (pH 6.5) and 25 mM KCl resulted in a significant increase in diameter (mean ± SE: 26.4 ± 5.2%) because of vesicle swelling as measured by confocal microscopy (Fig. 4). Under similar conditions, Mas 17, the inactive mastoparan analog, had no effect on vesicle size (mean ± SE: 3.41 ± 2.82%). These studies demonstrate that the ZG-associated $G_{\alpha i3}$ mediates GTP effect(s) on vesicle swelling.

Mas7 and GTP Influence on ZG Size Is KCl-Sensitive. When isolated ZGs were exposed to GTP or Mas7 in the absence of KCl (100 mM Mes buffer, pH 6.5/25 mM cyclamide), no increase in vesicle size was detected (data not shown). These results suggest that $G_{\alpha i3}$ may mediate GTP effects on vesicle swelling via the ZG-associated Cl^- and K^+ channels.

NaF and Mas7 Potentiate ZG Swelling to the Same Extent as GTP. Exposure of isolated ZG to 100 μM NaF for 10 minutes resulted in a 18–22% increase in vesicle diameter (mean ± SE: 20.85 ± 1.94%) as determined by confocal microscopy (Fig. 4). No increase in vesicle size was observed when ZGs incubated in KCl-free buffer (100 mM Mes buffer, pH 6.5/25 mM cyclamide) were exposed to the NaF, suggesting that, like the effect of Mas7 and GTP, the effect of NaF on ZG size is KCl-sensitive. Mas7, NaF, and GTP potentiated vesicle swelling similarly, suggesting that only ZG-associated heterotrimeric GTP-binding proteins participate in regulating ZG size.

Ca^{2+} Has no Influence on Vesicle Size. When isolated ZGs plated on Cell-Tak-coated mica sheets were placed in 100 mM Mes buffer (pH 6.5) and 25 mM KCl and exposed to either 100 μM Ca^{2+} or 200 μM EGTA, no significant effect on vesicle size was seen with up to 60 minutes of exposure (Fig. 4). Calcium buffers were formulated by a computer program developed by World Precision Instruments, (New Haven, CT) (30). AFM measurements of the ZG height expressed as a percentage of control after exposure of ZGs to 100 μM Ca^{2+} for 10 minutes showed a mean ± SE of 93.61 ± 3.81%. Similarly, exposure of ZGs to 200 μM EGTA for 10 minutes showed no significant change in height expressed as a percentage of control (mean ± SE of 103.46 ± 4.2%).

DISCUSSION

Results from the present study demonstrate association of the GTP-binding $G_{\alpha i3}$ protein with ZGM. The potentiation of vesicle swelling by GTP in these studies was most likely mediated through the $G_{\alpha i3}$ protein, regulating both the ZGM-associated Cl^- and K^+ channels (Fig. 5). The role of $G_{\alpha i3}$ protein in regulation of secretory vesicle volume may be key in regulating vesicle fusion at the cell plasma membrane. NaF, Mas7, and GTP promote increase in ZG size similarly, so only ZG-associated heterotrimeric GTP-binding proteins may be involved in the regulation of ZG size. Monomeric low molecular weight GTP-binding proteins associated with ZGM (17–19), on the other hand, may influence secretory vesicle targeting and docking rather than regulating vesicle volume and fusion at the plasma membrane. Furthermore, results from the present study support fluorimetric ZG and plasma membrane fusion assays (21), in which GTP and NaF were found to potentiate vesicle fusion but calcium had no effect. This nonresponsiveness of ZGs to Ca^{2+} in our study suggests that vesicle volume increase, a critical component in vesicle fusion at the plasma membrane, is Ca^{2+}-insensitive in pancreatic acinar cells. In response to a secretagogue, there is a transient increase in intracellular Ca^{2+} in acinar cells leading to exocytosis (39, 40). Exactly how Ca^{2+} is involved in exocytosis is little understood. Several studies in neurons and in neuroendocrine cells suggest Ca^{2+} to be involved in the fusion of secretory vesicles at the plasma membrane (41–44). In acinar cells, Ca^{2+} may not be involved in actual fusion of secretory vesicles at the plasma membrane but may play an important role in facilitating the release of vesicular contents after vesicle fusion, analogous to the role of Ca^{2+} proposed in rat mast cells (45).

From the present study, the presence and regulatory role of other ZG-associated G_i protein(s) in vesicle swelling and fusion cannot be ruled out. However, because $G_{\alpha i3}$ has been implicated in regulation of both the Cl^-- and ATP-sensitive K^+ channels in other tissues (22–25), it is very likely that the ZGM-associated $G_{\alpha i3}$ protein may be a major, if not the only, regulator of ZG swelling. However, this remains to be seen. Furthermore, as suggested in a recent study (46), the possibility that secretory vesicles matrices contain weak ion exchange resins that participate in the storage and release of secretory products has to be examined in ZG swelling.

We thank Gerhard H. Giebisch, Joseph F. Hoffman, Dana K. Andersen, and Ronald C. Merrell for valuable advice and discussion. This work was supported by grants from the National Institute of Health and the Ohse Award (to B.P.J), the National Institute of Health and the Whitaker Foundation (to J.P.G), and a postdoctoral fellowship from the Deutsche Forschungsgemeinschaft (to S.W.S).

1. Finkelstein, A., Zimmerberg, J. & Cohen, F. S. (1986) *Annu. Rev. Physiol.* **48,** 163–174.
2. Holz, R. W. (1986) *Annu. Rev. Physiol.* **48,** 175–189.
3. Almers, W. (1990) *Annu. Rev. Physiol.* **52,** 607–624.
4. Fernandez, J. M., Villalon, M. & Verdugo, P. (1991) *Biophys. J.* **59,** 1022–1027.
5. Curran, M. J. & Brodwick, M. S. (1991) *J. Gen. Physiol.* **98,** 771–790.

6. Monck, J. R., Oberhauser, A. F., Alverez de Toledo, G. & Fernandez, J. M. (1991) *Biophys. J.* **59,** 39–47.
7. Alverez de Toledo, G., Fernandez-Chacon, R. & Fernandez, J. M. (1991) *Nature* **363,** 554–558.
8. Gasser, K. W., DiDomenico, J. & Hopfer, U. (1988) *Am. J. Physiol. Gastroenterol.* **254,** G93–G99.
9. Fuller, C. M., Eckhardt, L. & Schulz, I. (1989) *Pfluegers Arch.* **413,** 385–394.
10. Fuller, C. M., Deetjen, H. H., Piiper, A. & Schulz, I. (1989) *Pfluegers Arch.* **415,** 29–36.
11. Gasser, K. W. & Hopfer, U. (1990) *Am. J. Physiol. Cell* **249,** C413–C420.
12. Thevenod, F., Gasser, K. W. & Hopfer, U. (1990) *Biochem. J.* **272,** 119–126.
13. Piiper, A., Plusczyk, T., Eckhardt, L. & Schulz, I. (1991) *Eur. J. Cell. Biol.* **54,** 322–330.
14. Thevenod, F., Chathadi, K. V. & Hopfer, U. (1992) *J. Memb. Biol.* **129,** 253–266.
15. Takuma, T., Ichida, T., Okumura, K., Sasaki, Y. & Kanazawa, M. (1993) *Am. J. Physiol.* **264,** G895–G901.
16. Thevenod, F., Hildebrandt, J-P., Striessnig, J., de Jong, H. R. & Schulz, I. (1996) *J. Biol. Chem.* **271,** 3300–3305.
17. Jena, B. P., Gumkowski, F. D., Konieczko, E. M., Fischer von Mollard, G., Jahn, R. & Jamieson, J. D. (1994) *J. Cell Biol.* **124,** 43–53.
18. Fischer von Mollard, G., Sudhof, T. C. & Jahn, R. (1991) *Nature (London)* **349,** 79–81.
19. Goud, B., Salminen, A., Walworth, N. C. & Novick, P. J. (1988) *Cell* **53,** 753–768.
20. Law, G. J., Northrop, A. J. & Mason, W. T. (1993) *FEBS Lett.* **333,** 56–60.
21. Nadin, C. Y., Rogers, J., Tomlinson, S. & Edwardson, J. M. (1989) *J. Cell Biol.* **109,** 2801–2808.
22. Kirsch, G. E., Codina, J., Birnbaumer, L. & Brown, A. M. (1990) *Am. J. Physiol.* **259,** H820–H826.
23. Ito, H., Tung, R. T., Sugimoto, T., Kobayashi, I. & Takahashi, K. (1992) *J. Gen. Physiol.* **99,** 961–983.
24. Schwiebert, E. M., Light, D. B., Fejes-Toth G., Naray-Fejes-Toth, A. & Stanton, B. A. (1990) *J. Biol. Chem.* **265,** 7725–7728.
25. Schwiebert, E. M., Kizer, N., Gruenert, D. C. & Stanton, B. A. (1992) *Proc. Natl. Acad. Sci. USA* **89,** 10623–10628.
26. Schneider, S. W., Sritharan, K. C., Geibel, J. P., Oberleithner H. & Jena, B. P. (1997) *Proc. Natl. Acad. Sci. USA* **94,** 316–321.
27. Hansma, P. K., Cleveland, J. P., Radmacher, M., Walters, D. A., Hillner, P. E., Bezanilla, M., Fritz, M., Vie, D., Hansma, H. G., Prater, C. B., Massie, J., Fukunaga, L., Gurley, J. & Elings, V. (1994) *Appl. Physiol. Lett.* **64,** 1738–1740.
28. Putman, C. A. J., Van der Werf, K. O., De Grooth, B. G., Van Hulst, N. F. & Greve, J. (1994) *Appl. Physiol. Lett.* **64,** 2454–2456.
29. Henderson, R. M., Schneider, S., Li, Q., Hornby, D., White, S. J. & Oberleithner, H. (1996) *Proc. Natl. Acad. Sci. USA* **93,** 8756–8760.
30. Jena, B. P., Padfield, P. J., Ingebritsen, T. S. & Jamieson, J. D. (1991) *J. Biol. Chem.* **266,** 17744–17746.
31. Cameron, R. & Castle, J. D. (1986) *J. Cell Biol.* **103,** 1299–1313.
32. Webster, P., Vanacore, L., Cohn, J. A. & Marino, C. (1993) *Am. J. Pathol.* **267,** C340–C348.
33. Bradford, M. M. (1976) *Anal. Biochem.* **72,** 248–254.
34. Macfarlane, D. E. (1988) *Anal. Biochem.* **176,** 457–463.
35. Konrad, R. J., Young, R. A., Record, R. D., Smith, R. M., Butkerait, P., Manning, D., Jarett, L. & Wolf, B. A. (1995) *J. Biol. Chem.* **270,** 12869–12876.
36. Higashijima, T., Uzu, S., Nakajima, T. & Ross, E. M. (1988) *J. Biol. Chem.* **263,** 6491–6494.
37. Vitale, N., Mukai, H., Rouot, B., Thiersé, D., Aunis, D. & Bader, M-F. (1993) *J. Biol. Chem.* **268,** 14715–14723.
38. Weingarten, R., Ransnäs, L., Mueller, H., Sklar, L. A. & Bokoch, G. M. (1990) *J. Biol. Chem.* **265,** 11044–11049.
39. Pandol, S. J., Schoeffield, M. S., Sachs, G. & Muallem, S. (1985) *J. Biol. Chem.* **260,** 10081–10086.
40. Kasai, H. & Augustine, J. G. (1990) *Nature (London)* **348,** 735–738.
41. Rastaad, M., Storm, J. F. & Andersen, P. (1992) *Eur. J. Neurosci.* **4,** 113–117.
42. Rosenmund, C., Clements, J. D. & Westbrook, G. L. (1993) *Science* **262,** 754–757.
43. Hessler, N. A., Shirke, A. M. & Malinow, R. (1993) *Nature (London)* **366,** 569–572.
44. Südhof, T. C. (1995) *Nature (London)* **375,** 645–653.
45. Fernández-Chac-n, R. & de Toledo, G. A. (1995) *FEBS Lett.* **363,** 221–225.
46. Parpura, V. & Fernandez, J. M. (1996) *Biophys. J.* **71,** 2356–2366.